COMPUTER GRAPHICS AND IMAGE PROCESSING (1974) 3, (277–299)

Determining Lightness from an Image

BERTHOLD K. P. HORN

Artificial Intelligence Laboratory, Massachusetts Institute of Technology, Cambridge, Massachusetts 02139

Communicated by P. H. Winston

Received June 10, 1974

A method for the determination of lightness from image intensity is presented. For certain classes of images, lightness corresponds to reflectance, while image intensity is the product of reflectance and illumination intensity. The method is two-dimensional and depends on the different spatial distribution of these two components of image intensity. Such a lightness-judging process is required for Land's retinex theory of color vision. A number of physical models are developed and computer simulation of the process is demonstrated. This work should be of interest to designers of image processing hardward, cognitive psychologists dealing with the human visual system and neurophysiologists concerned with the function of structures in the primate retina.

LIGHTNESS: DEFINITION

"The relative degree to which an object reflects light."

The Random House Dictionary

"The attribute of object colors by which the object appears to reflect or transmit more or less of the incident light."

Webster's Seventh New Collegiate Dictionary

1. REVIEW

1.1. *Theories of Color Perception*

There has always been great interest in how we perceive colors and numerous explanations have been forwarded [1–6]. A selection of some of the early works on this subject can be found in [7]. The human perceptual apparatus is remarkably successful in coping with large variations in illumination. The colors we perceive are closely correlated with the surface colors of the objects viewed, despite large temporal and spatial differences in color and intensity of the incident light. This is surprising since we cannot sense reflectance directly.

The light intensity at a point in the image is the product of the reflectance at the corresponding object point and the intensity of illumination at that point, aside from a constant factor that depends on the optical arrangement. There must then be some difference between these two components of image intensity which allows us to discount the effect of one. The two components differ in their spatial distribution. Incident light intensity will usually vary smoothly, with no discontinuities, while reflectance will have

sharp discontinuities at edges where objects adjoin. The reflectance is relatively constant between such edges.

1.1.1. *Tristimulus Theory*

Some facts about how we see color are fairly well established. It appears that we have three kinds of sensors (operating in bright illumination), with peak sensitivities in different parts of the visible spectrum. This is why it takes exactly three colors in additive mixture to match an unknown color. While it is difficult to determine the sensitivity curves of the three sensors directly, a linear transform of these curves has been known accurately for some time [8]. These curves, called the standard observer curves, are sufficient to allow one to predict color matches made by subjects with normal color vision [9].

The simplest theory of color perception then amounts to locally comparing the outputs of three such sensors and assigning color on this basis [3,5]. This, however, totally fails to explain the observed color constancy. Perceived color does not depend directly on the relative amounts of light measured by the three sensors [10,11].

1.1.2. *Color Conversion*

A number of attempts have been made to patch up this theory under the rubrics of "discounting of the illuminant," "contrast effect adjustment," and "adaptation." The more complicated theories are based on models with large numbers of parameters which are adjusted according to empirical data [12–16]. These theories are at least partially effective in predicting human color perception when applied to simple arrangements of stimuli similar to those used in determining the parameters.

The parameters depend strongly on the data and slight experimental variations will produce large fluctuations in them. This phenomenon is a familiar one to the numerical analyst and is expected whenever functions of many parameters are fitted to data. These theories are lacking in parsimony and convincing physiological counterparts. Lettvin has demonstrated the hopelessness of trying to find fixed transformations from locally compared outputs of sensors to perceived color [11].

1.2 *Land's Retinex Theory*

Another theory of color perception is embodied in Land's retinex model [10,17,18]. Land proposes that the three sets of sensors are not connected locally, but instead are treated as if they represent points on three separate images. Processing is performed on each such image separately to remove the component of intensity due to illumination gradient. Such processing is not merely an added frill but is indispensible to color perception in the face of the variability of illumination.

1.2.1. *Lightness Judging*

In essence a judge of lightness processes each image. Lightness is the perceptual quantity closely correlated with surface reflectance. Only after this

process can the three images be compared to reliably determine colors locally. It remains to mechanize this process. It would appeal to intuition if this process could be carried out in a parallel fashion that does not depend on previous knowledge of the scene viewed. This is because colors are so immediate, and seldom depend on one's interpretation of the scene. Colors will be seen even when the picture makes no sense in terms of previous experience. Also, color is seen at every point in an image.

1.2.2. *Miniworld of Mondrians*

In developing and explaining his theory Land needed to postpone dealing with the full complexity of arbitrary scenes. He selected a particular class of objects as inputs, modelled after the paintings of the turn-of-the-century Dutch artist Pieter Cornelis Mondrian. These scenes are flat areas divided into subregions of uniform matte color. Problems such as those occasioned by shadows and specular reflection are avoided in this way. One also avoids shading; that is, the variation in reflectance with the orientation of the surface with respect to the sensor and the light-source [19]. For Mondrians, lightness is considered to be a function of reflectance.

Mondrians are usually made of polygonal regions with straight sides; for the development here, however, the edges may be curved. In the world of Mondrians the reflectance has sharp discontinuities wherever regions meet and is constant inside each region. The illumination, on the other hand, varies smoothly over the image.

1.3. *Why Study the One-Dimensional Case?*

Images are two-dimensional and usually sampled at discrete points. For historic reasons and intuitive simplicity the results will first be developed in one dimension, that is with functions of one variable. Similarly, continuous functions will be used at first since they allow a cleaner separation of the two components of image intensity and illustrate more clearly the concepts involved.

Use will be made of analogies between the one-dimensional and two-dimensional cases as well as the continuous and discrete ones. The final process discussed for processing image intensities is two-dimensional and discrete. A number of physical implementations for this scheme are suggested. The process will be looked at from a number of points of view: partial differential equations, linear systems, Fourier transforms and convolutions, difference equations, iterative solutions, feed-back schemes and physical models.

1.3.1. *Notation*

The following notation will be used.

s': intensity of incident illumination at a point on the object
r': reflectance at a point on the object
p': intensity at an image point; product of s' and r'

s, r, p: Logarithms of s', r' and p', respectively

d: result of applying forward or differencing operator to p
t: result of applying threshold operator to d
l: result of applying inverse or summing operator to t

D: simple derivative operator in one dimension
T: continuous threshold operator, discards finite part
I: simple integration operator in one dimension
L: laplacian operator–sum of second partial derivatives
G: inverse of the Laplacian, convolution with $(1/2\pi) \log_e(1/r)$

$D*$, $T*$, $I*$, $L*$ and $G*$: discrete analogues of D, T, I, L, and G

The output l will not be called lightness since there is probably not yet a generally accepted definition of this term. It is, however, intended to be monotonically related to lightness. Note that l is related to the logarithm of reflectance, while the perceptual quantity is perhaps more closely related to the square root of reflectance.

1.4 *One-Dimensional Method–Continuous Case*

Land invented a simple method for separating the image components in one dimension. First one takes logarithms to convert the product into a sum. This is followed by differentiation. The derivative will be the sum of the derivatives of the two components. The edges will produce sharp pulses of area proportional to the intensity steps between regions, while the spatial

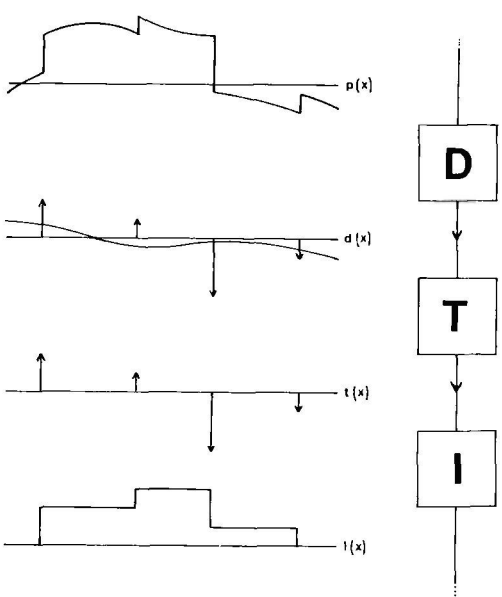

FIG. 1. Processing steps in the one-dimensional continuous case.

variation of illumination will produce only finite values everywhere. Now if one discards all finite values, one is left with the pulses and hence the derivative of lightness. Finally one undoes the differentiation by simple integration.

1.4.1. *One-Dimensional Continuous Method: Details*

We have the following: Let $r'(x)$ be the reflectance of the object at the point corresponding to the image point x. Let $s'(x)$ be the intensity at this object point. Let $p'(x)$ be their product, that is, the intensity recorded in the image at point x, Note that $s'(x)$ and $r'(x)$ are positive.

$$p'(x) = s'(x) * r'(x).$$

Now let $p(x)$ be the logarithm of $p'(x)$ and so on.

$$p(x) = s(x) + r(x).$$

Note that $s(x)$ is continuous and that $r(x)$ has some finite discontinuities. Let D represent differentiation with respect to x.

$$d(x) = D(p(x)) = D(s(x)) + D(r(x)).$$

Now $D(s(x))$ will be finite everywhere, while $D(r(x))$ will be zero aside from a number of pulses which carry all the information. Each pulse will correspond to an edge between regions and have area proportional to the intensity step. If now one "thresholds" and discards all finite parts, one gets

$$t(x) = T(D(p(x))) = D(r(x)).$$

To obtain $r(x)$ one only has to invert the differentiation, that is, integrate. Let I represent integration with respect to x, then $(I)^{-1} = D$ and

$$I(x) = I(T(D(p(x)))) = r(x) + c.$$

One can give a convolutional interpretation to the above, since differentiation corresponds to convolution with a pulse-pair, one negative and one positive, each of unit size. Integration corresponds to convolution with the unit-step function.

1.4.2. *Normalization*

The result is not unique because of the constant introduced by the integration. The zero (spatial) frequency term has been lost in the differentiation, so cannot be reconstructed. This is related to the fact that one does not know the overall level of illumination and hence cannot tell whether an object appears dark because it is grey or because the level of illumination is low.

One can normalize the result if one assumes that there are no light sources in the field of view and no fluorescent colors or specular reflections. This is certainly the case for the Mondrians. Perhaps the best way of normalizing the result is to simply assume that the highest value of lightness corresponds

to white, or total reflectance in the lambertian sense. This normalization will lead one astray if the image does not contain a region corresponding to a white patch in the scene, but this is the best one can do. Other normalization techniques might involve adjusting weighted local averages, but this would then no longer amount to reconstruction of reflectance.

1.5. *One-Dimensional Method–Discrete Case*

So far we have assumed that the image intensity was a continuous function. In retinas found in animals or artificial ones constructed out of discrete components, images are only sampled at discrete points. So one has to find discrete analogues for the operations we have been using. Perhaps the simplest are first differences and summation as analogues of differentiation and integration respectively. This is not to say that other approximations could not be used equally well.

To use the new operators, one goes through essentially the same process as before, except that now all values in the differenced image are finite. This has the effect of forcing one to choose a threshold for the thresholding function. Both components of image intensity produce finite values after the differencing operation. The component due to the edges in the reflectance is hopefully quite large compared to that due to illumination gradient. One has to find a level that will suppress the illumination gradient inside regions, while permitting the effects due to edges to remain.

1.5.1. *One-Dimensional Discrete Method: Details*

Let r'_i be the reflectance of the object at the point corresponding to the image point i. Let s'_i be the incident light intensity at this object point. Let p'_i be their product, that is, the intensity in the image at point i.

$$p'_i = s'_i * r'_i.$$

Now let p_i be the logarithm of p'_i, and so on. Let $D*$ and $I*$ be the operators corresponding to taking first differences and summation respectively. Note that $(I*)^{-1} = D*$.

$$p_i = s_i + r_i,$$
$$d_i = p_{i\ 1} - p_i \quad (d = D*(p)),$$
$$t_i = d_i \text{ if } |d_i| > e, \text{ else } 0,$$
$$l_i = \sum_{k=0}^{i} t_k \qquad (l = I*(t)).$$

1.5.2. *Selecting the Threshold*

How shall we select the threshold? It must be smaller than the smallest intensity step between regions. It must on the other hand be larger than values produced by first differencing the maximum illumination gradients. Real images are noisy and the threshold should be large enough to eliminate this noise inside regions.

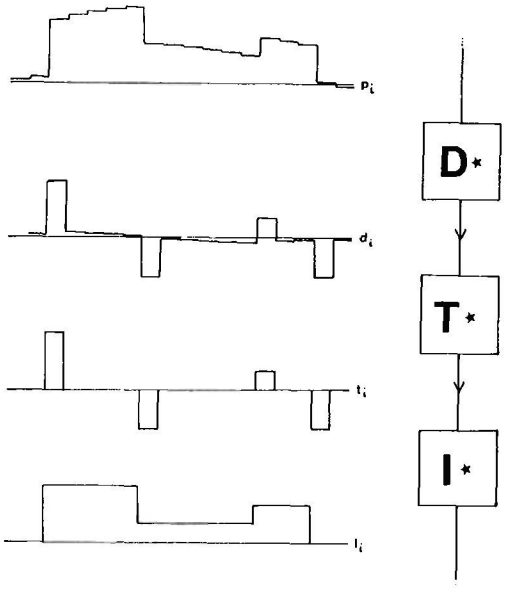

FIG. 2. Processing steps in the one-dimensional discrete case.

The spacing of the sensor cells must also be taken into account. As this spacing becomes smaller, the contribution due to illumination gradients decreases, while the component due to the edges remains constant. A limit is reached when the component due to illumination gradients falls below that due to noise or when the optical properties of the imaging system begin to have a deleterious effect. In all imaging systems an edge is spread over a finite distance due to diffraction and uncorrected abberations. The spacing of sensors should not be much smaller than this distance to avoid reducing the component due to edges in the differenced image.

Let u be the radius of the point-spread-function of the optical system and h the spacing of the sensor cells. Let g' be the smallest step in the logarithm of reflectance in the scene. Then define the effective minimum step (in p) as

$$g = g' * \min(1, h/2u).$$

Let α be the largest slope due to illumination gradient and σ the root-mean-square noise-amplitude. The noise will exceed a value 3σ only 0.3% of the time. Choose the threshold e as follows.

$$e < g,$$
$$e > \alpha h,$$
$$e > 3\sqrt{2}\,\sigma.$$

1.5.3. *Accuracy of the Reconstruction*

In the continuous case one can exactly reconstruct the reflectance, aside from a constant. We are not so fortunate here, even if we select a threshold

according to the above criteria. This is because the values at the edges contain small contributions due to illumination gradient and noise. A slight inaccuracy in the reconstruction will result. This error is minimized by making the sensor-cell spacing very fine, optimally of a size commensurate with the optical resolution of the device. The effect of noise can also be minimized by integrating over time.

Note that the reconstruction is more accurate when there are few edges, since it is at the edges that the error effects appear. With many edges the illumination gradient begins to "show through."

1.5.4. *Generalizations*

So far we have dealt with constant sensor spacing. Clearly as long as the same spacing is used for both the differencing and the summing, the cell spacing can be arbitrary and has little effect on the reconstruction since it does not enter into the equations.

Similarly we have chosen first differences as the discrete analogue for differentiation. We could have chosen some other weighted difference and developed a suitable inverse for it. This inverse of course would no longer be summation, but can be readily obtained using techniques developed for dealing with difference equations [20,21].

1.5.5. *Physical Models of the One-Dimensional Discrete Process*

One can invent a number of physical models of the above operations. A simple resistive network will do for the summation process, for example. Land has implemented a small circular "retina" with about 16 sensors [18]. This model employs electronic components to perform the operations of taking logarithms, differencing, thresholding, and summing.

Land has tried to extend his one-dimensional method to images, by covering the image with paths produced by a random-walk procedure and applying methods like the above to each of these paths. While this produces results, it seems unsatisfactory from the point of view of suggesting possible neurophysiological structures; neither does it lend itself to efficient implementation.

Methods depending on nonlinear processing of the gradient along paths in the image fail to smoothly generalize to two dimensions, and do not predict the appearance of images in which different paths result in different lightnesses.

2. LIGHTNESS IN TWO-DIMENSIONAL IMAGES

2.1. *Two-Dimensional Method–Continuous Case*

We need to extend our ideas to two dimensions in order to deal with actual images. There are a number of ways of arriving at the process to be described here, we shall follow the simplest [22]. One needs to find two-dimensional analogues to differentiation and integration. The first partial derivatives are directional and thus unsuitable since they will, for example,

completely eliminate evidence of edges running in a direction parallel to their direction of differentiation. Exploring the partial derivatives and their linear combinations one finds that the laplacian operator is the lowest order combination that is isotropic, or rotationally symmetric. The laplacian operator is, of course, the sum of the second partial derivatives.

2.1.1. *Applying the Laplacian to a Mondrian*

Before investigating the invertibility of this operator, let us see what happens when one applies it to the image of a Mondrian. Inside any region one will obtain a finite value due to the variation in illumination intensity. At each edge one will get a pulse pair, one positive and one negative. The size of each pulse will be equal to the intensity step.

This can best be seen by considering the first derivative of a step, namely a single pulse. If this is differentiated again, one obtains a doubled pulse as described. Since this pulse will extend along the edge, one may think of it as a pulse-wall. So each edge separating regions will produce a doubled pulse-wall. It is clear that one can once again separate the component due to reflectance and illumination simply by discarding all finite parts.

2.1.2. *Inverse of the Laplacian Operator*

To complete the task at hand one then has to find a process for undoing the effect of applying the laplacian. Again there are a number of approaches to this problem, we will use the shortest [22]. In essence one has to solve for $p(x,y)$ in a partial differential equation of the form

$$L(p(x,y)) = d(x,y).$$

This is Poisson's equation, and it is usually solved inside a bounded region using Green's function [21].

$$p(x,y) = \int\int G(\xi,\eta;x,y)\ d(\xi,\eta)\ d\xi\ d\eta.$$

The form of Green's function G, depends on the shape of the region boundary. If the retina is infinite all points are treated similarly and Green's function depends only on two parameters, $(\xi - x)$ and $(\eta - y)$. This positional independence implies that the above integral simply becomes a convolution. It can be shown that Green's function for this case is:

$$G(\xi,\eta;x,y) = (1/2\pi)\ \log_e(1/r),$$

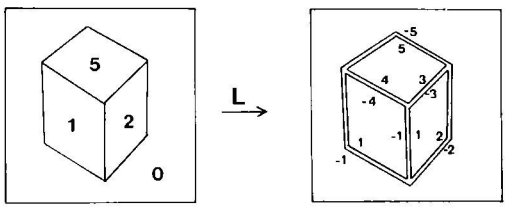

FIG. 3. Applying the laplacian operator to the image of a Mondrian figure.

Where

$$r^2 = (\xi - x)^2 + (\eta - y)^2.$$

So

$$p(x,y) = \int\int (1/2\pi) \log_e(1/r)\, d(\xi,\eta)\, d\xi\, d\eta.$$

Thus the inverse of the laplacian operator is simply convolution with $(1/2\pi) \log_e(1/r)$. To be precise one has

$$\left(\frac{\partial^2}{\partial x^2} + \frac{\partial^2}{\partial y^2}\right) \int\int (1/2\pi) \log_e(1/r)\, d(\xi,\eta)\, d\xi\, d\eta = d(x,y).$$

This is a two-dimensional analogue of

$$\frac{d}{dx} \int_{-\infty}^{x} f(t)\, dt = f(x).$$

2.1.3. *Why One Can Use the Convolutional Inverse*

If the retina is considered infinite one can express the inverse as a simple convolution. If the retina is finite, on the other hand one has to use the more complicated Green's function formulation.

Now consider a scene on a uniform background and assume that the image of the scene is totally contained within the retina. The result of applying the forward transform and thresholding will be zero in the area of the uniform background. The convolutional inverse will therefore receive no contribution from outside the retina. As a result one can use the convolutional form of the inverse provided the image of the scene is totally contained within the retina.

2.1.4. *Normalization*

Once again one finds that the reconstructed reflectance is not unique. That is, any nonsingular solution of $L(p(x,y)) = 0$ can be added to the input without affecting the result. On the infinite plane such solutions have the form $p(x,y) = (ax + by + c)$. If the scene only occupies a finite region of space it can be further shown that the solution will be unique up to a constant and that one does not have to take account of possible slopes. To be specific, the background around the scene will be constant in the reconstruction. So one has here exactly the same normalization problem as in the one-dimensional case. Calling the region with highest numerical value white appears to be a reasonable method.

2.1.5. *Two-Dimensional Continuous Method: Details*

Let $r'(x,y)$ be the reflectance of the object at the point corresponding to the image point (x,y). Let $s'(x,y)$ be the source intensity at that object point. Let $p'(x,y)$ be their product, that is, the intensity at the image point (x,y). Note that $r'(x,y)$ and $s'(x,y)$ are positive.

$$p'(x,y) = s'(x,y) * r'(x,y).$$

Let $p(x,y)$ be the logarithm of $p'(x,y)$ and so on:

$$p(x,y) = s(x,y) + r(x,y).$$

Now assume that $s(x,y)$ and its first partial derivatives are continuous, a reasonable assumption to make for the distribution of illumination on the object. Let L be the laplacian operator.

$$d(x,y) = L(p(x,y)) = L(s(x,y)) + L(r(x,y)).$$

Now $L(s(x,y))$ will be finite everywhere, while $L(r(x,y))$ will be zero except at each edge separating regions, where one will find a double pulse wall as described. Now discard all finite parts

$$t(x,y) = T(L(p(x,y))) = L(r(x,y)).$$

Let G be the operator corresponding to convolution by $(1/2\pi)\log_e(1/r)$. Note that $(G)^{-1} = L$.

$$l(x,y) = G(T(L(p(x,y)))) = r(x,y) + c.$$

2.2. *Two-Dimensional Method–Discrete Case*

Once again we turn from a continuous image to one sampled at discrete points. First we will have to decide on a tesselation of the image plane.

2.2.1. *Tesselation of the Image Plane*

For regular tesselations the choice is between triangular, square, and hexagonal unit cells. In much past work on image processing, square tesselations have been used for the obvious reasons. This particular tesselation of the image has a number of disadvantages. Each cell has two kinds of neighbors, four adjoining the sides, four on the corners. This results in a number of asymmetries. It makes it difficult, for example, to find convenient difference schemes approximating the laplacian operator with low error term.

Triangular unit cells are even worse in that they have three kinds of neighbors, compounded these drawbacks. Note also that near-circular objects pack tightest in a pattern with hexagonal cells. For these reasons we will use a hexagonal unit cell. It should be kept in mind however that it is easy to develop equivalent results using different tesselations.

2.2.2. *Discrete Analogue of the Laplacian*

Having decided on the tesselation we need now to find a discrete analogue of the laplacian operator. Convolution with a central positive value and a rotationally symmetric negative surround of equal weight is one possibility. Aside from a negative scale factor, this will approach application of the Laplacian in the limit as the cell size tends to zero.

If one were to use complicated surrounds, the trade-offs between accuracy and resolution would suggest using a negative surround that decreases rapidly outward. For the sake of simplicity we will choose convolution with a

central cell of weight one, surrounded by six cells of weight $-\frac{1}{6}$. This function is convenient, symmetric, and has a small error term. It is equal to $-(h^2/4)L - (h^4/64)L^2$ plus sixth- and higher-order derivatives [20]. It should again be pointed out that similar results can be developed for different functions.

2.2.3. *Inverse of the Discrete Operator*

The forward differencing operator has the form

$$d_{ij} = p_{ij} - \Sigma\, w_{k-i,l-j}\, p_{kl}.$$

Where p_{ij} is the logarithm of image intensity, w_{ij} are weights, which in our case are $\frac{1}{6}$, and the sum is taken over the six immediate neighbors.

We now have to determine the inverse operation that recovers p_{ij} from d_{ij}. One approach is to try and solve the difference equation of the form

$$p_{ij} - \Sigma\, w_{k-i,l-j}\, p_{kl} = d_{ij}.$$

Or in matrix form: $W\,\mathbf{p} = \mathbf{d}$. Note that W is sparse, having 1's on the diagonal and $-\frac{1}{6}$'s scattered around. For a finite retina with n sensor cells one has to introduce boundary conditions to ensure that one has as many equations as there are unknowns. One then simply inverts the matrix W and gets: $\mathbf{p} = W^{-1}\,\mathbf{d}$.

This is entirely analogous to the solution in the continuous case for a finite retina. W^{-1} corresponds to the Green's function. Much as Green's function has a large "support," that is, is nonzero over a large area, so W^{-1} is not sparse. This implies that a lot of computation is needed to perform the inverse operation.

2.2.4. *Computational Effort and Simplification*

Solving the difference equations for a given image by simple Gauss–Jordan elimination requires of the order of $n^3/2$ arithmetic operations. An-

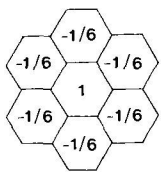

FIG. 4a. A discrete analogue of the laplacian operator.

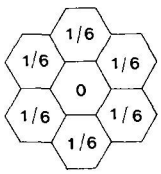

FIG. 4b. Delta function minus this discrete analogue.

other approach is to invert W once and for all for a given retina. For each image then one needs only about n^2 arithmetic operations. Note that the other operations, such as forward differencing, require only about $6n$ arithmetic operations.

What in effect is happening is that each point in the output depends on each point in the differenced image. Both have n points, so n^2 operations are involved. Not only does one have to do a great deal of computation, but must also store up the matrix W^{-1} of size n^2. This is quite prohibitive for even a small retina.

This latter problem can be avoided if one remembers the simplification attendant to the use of an infinite retina in the continuous case. There we found that the integral with Green's function simplified into a convolution. Similarly, if one assumes an infinite retina here, one finds that W and its inverse become very regular. The rows in W are then all the same and the same is true of W^{-1}. Each value in the output depends in the same way on the neighboring points in the differenced image. For this simple convolutional operation one need only store up the dependence of one point on its neighbors.

The only remaining difficulty is that W is now infinite and one can no longer invert it numerically; one has to find an analytical expression for the inverse. I have not been able to find this inverse exactly. A good first approximation is $\log_6(r_0/r)$ – except for $r = 0$, when one uses $1 + \log_6(r_0)$. Here r is the distance from the origin and r_0 is arbitrary. The remainder left over when one applies the forward difference scheme to this approximation lies between $\log_6(1 + r^{-6})$ and $\log_6(1 - r^{-6})$. This error term is of the order of r^{-6}.

In practice one does not have an infinite retina, but as has been explained for the continuous case, one can use the convolutional method described above for a finite retina, provided that the image of the scene is wholly contained within the retina. It is possible to find an accurate inverse of this kind valid for a limited retinal size by numerical means.

2.2.5. *Two-Dimensional Discrete Method: Details*

Let r'_{ij} be the reflectance at the object point corresponding to the image point (i,j). Let s'_{ij} be the intensity of the incident light at this object point. Let p'_{ij} be the intensity in the image at point (i,j).

$$p'_{ij} = s'_{ij} * r'_{ij}.$$

Let p_{ij} be the logarithm of p'_{ij} and so on. Let $L*$ be the operator that corresponds to convolution with the analogue of the Laplacian. Let $G*$ be its inverse.

$$p_{ij} = s_{ij} + r_{ij},$$
$$d_{ij} = p_{ij} - \Sigma w_{k-i,l-j}\, p_{kl} \quad (d = L*(p)).$$

The weights w_{ij} are $\frac{1}{6}$ in this case, and the sum is taken over the six immediate neighbors.

$$t_{ij} = d_{ij} \text{ if } |d_{ij}| > e, \text{ else } 0,$$
$$l_{ij} = \Sigma v_{k-i,l-j}\, t_{kl} \qquad (l = G*(t)).$$

Here the sum extends over the whole retina and v_{ij} is the convolutional inverse found numerically as explained above.

2.2.6. *Simplicity of the Inverse*

The forward transform, involving only a simple subtraction of immediate neighbors, is clearly a rapid, local operation. The inverse on the other hand is global, since each point in the output depends on each point in the differenced image. Computationally this makes the inverse slow. The inverse is simple in one sense, however: The difference equations being solved by the inverse have the same form as the equations used for the forward transform and are thus local. The problem is that the output here feeds back into the system and effects can propagate across the retina. The apparent global nature of the inverse is thus of a rather special kind and, as we will see later, gives rise to very simple physical implementations involving only local connections.

2.2.7. *Iterative Methods of Solution*

There are, of course, other methods for solving large sets of equations. The fact that W is sparse and has large diagonal elements, suggests trying something like Gauss–Seidel iteration. Each iteration takes about $6n$ arithmetic operations. For effects to propagate across the retina one requires at least $((4n^2 - 1)/3)^{1/2}$ iterations. This is because a hexagonal retina of width m has $(3m^2 + 1)/4$ cells. The above suggests that one might be able to get away with less than n^2 arithmetic operations. In practice it is found that effects propagate very slowly and many more iterations are needed to stabilize the solution. One does not have to store W, since it is easily generated as one goes along.

Iterative schemes correspond to adding a time-derivative to the Poisson equation and so turning it into a heat-equation. As one continues to iterate, the steady-state solution is approached. This intuitive model gives some insight into how the process will converge.

2.2.8. *Convergence of Iterative and Feedback Schemes*

If iterative schemes of solving the difference equations converge, they will converge to the correct solution. It is, however, not immediately obvious that they will converge at all. Let δ be the delta function, that is, one at the origin, zero elsewhere. It can be shown that if the forward convolutional operator is w, the convergence of iterative schemes depends on the behaviour of the error term, $(\delta - w)^n$, as n becomes large. Raising a convolutional operator to an integer power is intended to signify convolution with itself.

In our case, w is one at the origin, with six values of $-\frac{1}{6}$ around it. So $(\delta - w)$ will be zero at the origin with six values of $\frac{1}{6}$ around it. Now while $(\delta - w)^n$ will always have a total area of one, it does spread out and its value tends to zero at every point as n tends to infinity. So this iterative scheme converges: Similar results can be derived for other negative surrounds.

2.2.9. *Setting the Threshold*

In the discrete case a finite threshold must be selected. As before, let g' be the smallest step in the logarithm of reflectance in the scene, h the sensor spacing, and u the radius of the point-spread function of the optical system. Then we define the effective minimum step (in p) as

$$g = g' * \min(1, h/2u).$$

There are some minor differences in what follows depending on whether one considers the sensor outputs to be intensity samples at cell-centers or averages over the cell area. The smallest output due to an edge will be about $g/6$. This is produced when the edge is oriented to cover just one cell of the neighborhood of six. Let β be the maximum of the intensity gradient; that is, the laplacian of intensity in this case. Choose the threshold e as follows

$$e < g/6,$$
$$e > \beta h^2,$$
$$e > 3(7/6)^{1/2}\sigma.$$

2.2.10. *Some Notes on This Method*

Notice that an illumination gradient that varies as some power of distance across the image becomes a linear slope after taking logarithms and thus produces no component after the differencing operations. Such simple gradients are suppressed even without the thresholding operation.

In practice the parameters used in choosing the threshold may not be known or may be variable. In this case one can look at a histogram of the differenced image. It will contain values both positive and negative corresponding to edges and also a large number of values clustered around zero due to illumination gradients, noise, and so on. The threshold can be conveniently chosen to discard this central blob.

Noise and illumination gradients have an effect similar to that in the one-dimensional case. With finite cell spacing, one cannot precisely separate the two components of the image intensity and at each edge the information will be corrupted slightly by noise and illumination gradient. As the density of edges per cell area goes up, the effect of this becomes more apparent. In highly textured scenes the illumination gradient is hard to eliminate.

Once again one has to decide on a normalization scheme. The best method probably is to let the highest numerical value in the reconstructed output correspond to white.

2.2.11. *Dynamic Range Reduction*

Applying the retinex operation to an image considerably reduces the range of values. This is because the output, being related to reflectance, will only have a range of one to two orders of magnitude, while the input will also have illumination gradients. This will make such processing useful for picture recording and transmission [22].

2.2.12. *A Frequency Domain Interpretation*

It may be of interest to look at this method from yet another point of view. What one does is to accentuate the high-frequency components, threshold and then attenuate the high-frequency components. To see this, consider first the forward operation. The Fourier transform of the convolutional operator corresponding to differentiation is $i\omega$. Similarly the two-dimensional Fourier transform of the convolutional operator corresponding to the laplacian is $-\rho^2$. Here ρ is the radius in a polar-coordinate system of the two-dimensional frequency space. In either case one is multiplying the fourier transform by some function that increases with frequency. Now consider the reverse operation. The fourier transform of the convolutional operation corresponding to integration is $1/i\omega$. Similarly the Fourier transform of $(1/2\pi)$ $\log_e(1/r)$ is $-1/\rho^2$. So in the inverse step one undoes exactly the emphasis given to high frequency components in the forward operation.

In both the one-dimensional and the two-dimensional case one loses the zero frequency component. This is why the result has to be normalized.

2.3. *Physical Models*

There are numerous continuous physical models to illustrate the inverse transformation. Anything that satisfies Poisson's equation will do. Such physical models help one visualize what the inverse of a given function might be. Examples in two dimensions are: perfect fluid-flow, steady diffusion, steady heat-flow, deformation of an elastic membrane, electro-statics and current flow in a resistive sheet. In the last model, for example, the input is the distribution of current flowing into the resistive sheet normal to its surface; the output is the distribution of electrical potential over the surface.

In addition to helping one visualize solutions, continuous models also suggest discrete models. These can be arrived at simply by cutting up the two-dimensional space in a pattern corresponding to the interconnection of neighboring cells. That is, the remaining parts form a pattern dual to that of the sensor cell pattern. We will discuss only one such discrete model.

2.3.1. *A Discrete Physical Model*

Consider the resistive sheet described, cut up in the dual pattern of the hexagonal unit cell pattern. What will be left is an interconnection of resistors in a triangular pattern. The inputs to this system will be currents injected at the nodes, the potential at the nodes being the output. This then provides a very simple analog implementation of the tedious inverse computation.

It is perhaps at first surprising to see that each cell is not connected to every other in a direct fashion. One would expect this from the form of the computational inverse. Each cell in the output does of course have a connective via the other cells to each of the inputs. Paths are shared however in a way that makes the result both simple and planar.

Consider for the moment just one node. The potential at the node is the

average of the potential of the six nodes connected to it plus the current injected times $R/6$, where R is the resistance of each resistor. The economy of connection is due to the fact that the outputs of this system are fed back into it. It also illustrates that this model locally solves exactly the same difference equation as that used in the forward transform, only now in reverse.

This immediately suggests an important property of this model. By simply changing the interconnections, one can make an inverse for other forward transforms. Simplest of all are other image-plane tesselations, both regular and irregular. One simply connects the resistors in the same pattern as are the cells in the input.

More complicated weighted surrounds can be handled by using resistors with resistances inversely proportional to the weights. The network of resistors will then no longer be planar.

2.3.2. *A Feedback Scheme for the Inverse*

Both the comment about outputs feeding back into the resistive model and the earlier notes about iterative schemes suggest yet another interesting model for the inverse using linear summing devices. Operational amplifiers can serve this purpose. One simply connects the summing elements so that they solve the difference equation implied by the forward transform. Once again it is clear that such a scheme can be generalized to arbitrary tesselations and weighted negative surrounds simply by changing the interconnections and attenuations on each input. Some questions of stability arise with esoteric interconnections. For the simple ones stability is assured.

A little thought will show that the resistive model described earlier is in fact a more economical implementation of just this scheme with the difference that there the inputs are currents, while here they are potentials.

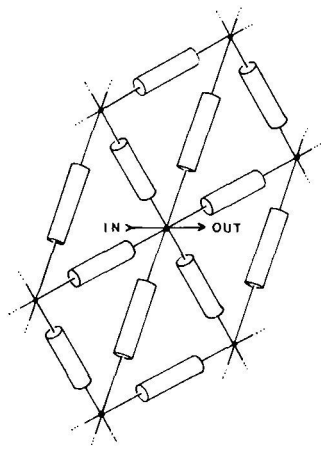

FIG. 5. Resistive model of the inverse computation. The inputs are the currents injected at the nodes. The outputs are the potentials at the nodes.

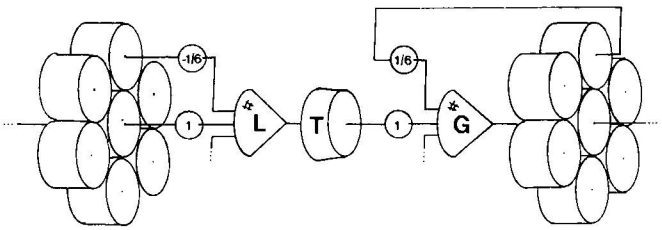

FIG. 6. The use of summing elements and feed-back in the implementation of both the forward and the inverse transform.

2.4. *Limitations of the Simple Scheme Presented*

The method presented here will not correctly calculate reflectance if used unmodified on general scenes. It may, however, calculate lightness fairly well. As the method stands now, for example, a sharp shadow edge will not be distinguished from a real edge in the scene and the two regions so formed will produce different outputs, while their reflectances are the same. It may be that this is reasonable nevertheless, since we perceive a difference in apparent lightness.

Smooth gradations of reflectance on a surface due either to shading or variations in surface reflectance will be eliminated by the thresholding operations except as far as they affect the intensity at the borders of the region. This may imply that we need additional channels in our visual system to complement the ones carrying the retinexed information since we do utilize shading as a depth-cue [19].

The simple normalization scheme described will also be sensitive to specular reflections, fluorescent paints and light-sources in the field of view. Large depth-discontinuities present another problem. One cannot assume that the illumination is equal on both sides of the obscuring edge. In this case the illuminating component does not vary smoothly over the retina, having instead some sharp edges.

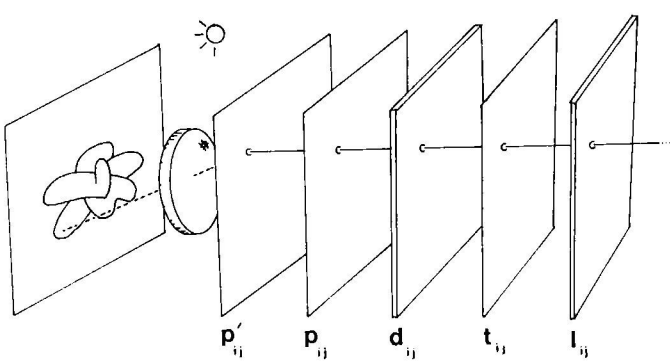

FIG. 7. Illustration of the parallel layers of operations which perform the two-dimensional retinex operation. Only two of the operations involve local interactions between neighboring cells.

2.5. *Computer Simulation of the Discrete Method*

A computer program was used to simulate the retinex process described on a small retina with both artificial images and images seen through an image dissector camera. The hexagonal unit-cell is used in this program and the retina itself is also hexagonal. The retina contains 1027 cells in a pattern 36 cells across. This is a compromise dictated by the need to limit the number of arithmetic operations in the inverse transform. In this case one needs about a million and this takes about a minute of central processor time on our PDP-10.

Both the artificial and the real Mondrians consist of regions bounded by curved outlines to emphasize that this method does not require straight-line edges or boundary extraction and description. Various distributions of incident illumination can be selected for the artificial scenes. In each case the processing satisfactorily removes the gradient.

For the real scenes it is hard to produce really large illumination gradients by positioning the light-sources. The reconstruction does eliminate the gradient well, but often minor flaws will appear in the output due to noise in the input and a number of problems with this kind of input device such as a very considerable scatter. It is not easy to predict what effects such imaging device defects will have.

The output is displayed on a DEC 340 display which has a mere eight grey-levels. It would be interesting to experiment with larger retinas and better image input- and output-devices.

2.5.1. *Form of Inverse used in the Computer Simulation*

The convolutional form of the inverse was used for speed and low storage requirement. This neccesitated solving the difference equations once, given a pulse as input. The symmetry of the hexagonal pattern allows one to identify symmetrically placed cells and only 324 unknowns needed to be found for a convolutional inverse sufficient for the size of retina described. As mentioned before, this function is closely approximated by $\log_6(r_0/r)$ for large r. This can be used to establish boundary conditions.

3. IMPLICATIONS AND CONCLUSIONS

3.1. *Parallel Image Processing Hardware*

The methods described here for forward transforming, thresholding and inverse transforming immediately tempt one to think in terms of electronic components arranged in parallel layers. Enough has been said about different models to make it clear how one might connect such components. Large scale integrated circuit technology may be useful, provided the signals are either converted from analog to digital form or better still, good linear circuits are available.

Construction of such devices would be premature until further experimentation is performed to decide on optimal tesselations, negative sur-

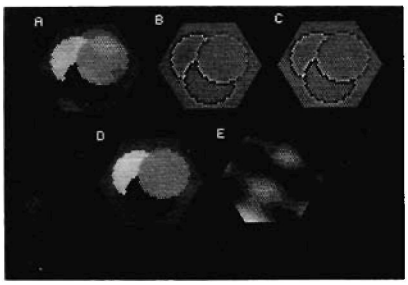

FIG. 8. The method applied to an artificial image.[1]

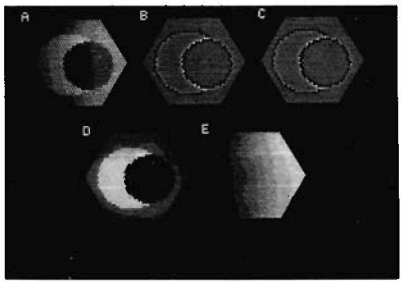

FIG. 9. The method applied to a real image.[1]

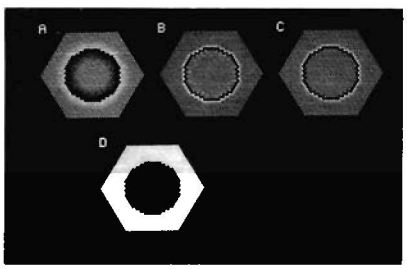

FIG. 10. The method applied to Craik's figure.[1]

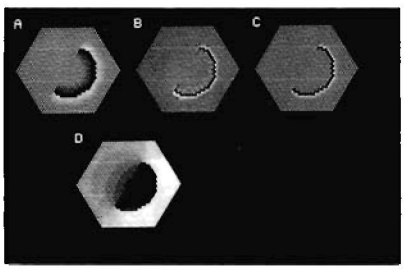

FIG. 11. Apparent lightness predicted for incomplete figure.[1]

rounds, thresholding operations and normalization schemes. These decisions are best guided by computer simulation.

3.2 *Cognitive Psychology*

One of the artificial scenes was created to illustrate Craik's illusion [8,23]. Here a sharp edge is bordered by second-order gradients. As one might expect, the smooth gradients are lost in the thresholding and reconstruction produces two regions each of uniform brightness. The difference in brightness between the regions is equal to the original intensity step at the edge.

The fact that the process presented here falls prey to this illusion is of course no proof that humans use the same mechanism. It is interesting, however, that this technique allows one to predict the appearance of pictures containing incompletely closed curves with second-order gradients on either side.

3.3. *Neurophysiology*

The method described here for obtaining lightness from image intensity suggests functions for a number of structures in the primate retina. The horizontal cells appear to be involved in the forward transformation, while some of the amacrines may be involved in the inverse transformation. For details,

[1] The subfigures in the above have the following interpretation. (A) p_{ij}, input–logarithm of image intensity; (B) d_{ij}, differenced image; (C) t_{ij}, thresholded difference; (D) l_{ij}, output–computed lightness; (E) s_{ij}, illumination distribution–$[p_{ij} - l_{ij}]$.

see the paper by Marr [24] in which he uses this hypothesis to explain an astonishing number of facts about the retina.

3.4. *Further Elaborations of the Model*

If the sensors are not equally sensitive, the outputs of the differencing stage will be offset. Such offsets can be eliminated by introducing the equivalent of ac coupling at this point. This will suppress constant offsets while permitting rapid changes to be reproduced with fidelity. Clearly now the output will fade away if the image is stabilized. Either large linear motion or small-scale jitter will prevent this. It is convenient to combine this coupling with the threshold operation. A signal then appears at the output of this stage only if a significant change happens in a time commensurate with the time constant of the coupling.

This presents not merely a mechanism for dealing with imperfect sensors. One kind of adaptation to overall changes in light levels, for example, can be envisioned as taking place at the earliest stage in the system, at the sensors themselves. Their outputs can always be proportional to the incident intensity, but the constant of proportionality would be adjusted to deal with varying light levels. This would lead to offsets at the output of the differencing stage and can be dealt with by the proposed coupling. An unfortunate side-effect of this arrangement is the appearance of after-images.

If one wishes to achieve dynamic range reduction beyond that possible by calculating reflectance one merely has to go "too far" in eliminating the illumination gradient. All that is necessary is that the difference and inverse operations are not exact inverses. Specifically, one can retain the same inverse operation but modify the differencing stage by allowing the total weight of the negative surround to exceed that of the central positive-pulse. The differenced signal now has a small additional negative component proportional to the image intensity. When passed through the inverse stage this produces additional smooth changes in the output. The output of such a system of course is no longer proportional to lightness and suffers from Mach-bands and simultaneous contrast effects.

3.5. *Conclusion*

A simple, layered, parallel technique for computing lightness from image intensity has been presented. The method does not involve an ability to describe or understand the scene, relying instead on the spatial differences in the distribution of reflectance and illumination. The forward step involves accentuating the edges between regions. The output of this step is then thresholded to remove illumination gradients and noise. The inverse step merely undoes the accentuation of the edges.

Physical models have been given which can perform this computation efficiently in parallel layers of simple networks. The method has been simulated and applied to a number of images. The method grew out of an attempt to extend Land's method to two dimensions and fills the need for a lightness-judging process in his retinex theory of color perception.

The possibility of processing an image in such a parallel, simple fashion without higher-level understanding of the scene reinforces my belief that such low-level processing is of importance in dealing with a number of features of images. Amongst these are shading, stereo disparity, focus, edge detection, scene segmentation and motion parallax. Some of this kind of processing may actually happen in the primate retina and visual cortex. The implication for image analysis may well be that a number of such preprocessing operations should be performed automatically for the whole image to accentuate or extract certain attributes before one brings to bear the more powerful, but tedious and slow sequential goal-directed methods.

ACKNOWLEDGMENTS

I wish to thank Dr. David Marr for a number of most interesting discussions and for encouraging me to commit this method to paper. He first observed that the primate retina appears to have just the right detailed structure to implement the functions here described.

Work reported herein was conducted at the Artificial Intelligence Laboratory, a Massachusetts Institute of Technology research program supported in part by the Advanced Research Projects Agency of the Department of Defense and monitored by the Office of Naval Research under Contract Number N00014-70-A-0362-0005.

REFERENCES

1. SIR ISAAC NEWTON, *Opticks*, Samuel Smith & Benjamin Walford, London, 1704. Also Dover, New York, 1952.
2. J. W. VON GOETHE, *Zur Farbenlehre*, Tuebingen, 1810. Also *Theory of Colours* translated by C. L. Eastlake, M.I.T. Press, Cambridge, Mass., 1970.
3. T. YOUNG, *On the Theory of Light and Color*, Philosophical Transactions, 1820. Also in *Color Vision* (R. C. Teevan and R. C. Birney, Eds.), Van Nostrand, Princeton, N.J., 1961.
4. J. C. MAXWELL, Theory of the Perception of Colors, *Transactions of the Royal Scottish Society of Arts* **4**, 394–400, 1856.
5. H. L. F. HELMHOLTZ, *Handbuch der Physiologischen Optik*, Voss, Leipzig, 1867. Also translated: J. P. C. S. Southall, *Handbook of Physiological Optics*, Dover, New York, 1962.
6. E. HERING, Zur Lehre vom Lichtsinne–Grunzuege einer Theorie des Farbsinnes, *SBK. Akad. Wiss. Wien Math. Naturwiss. K.* **70**, 1875. Also *Outlines of a Theory of the Light Sense*, translated by L. M. Hurrich and D. Jameson, Harvard Univ. Press, Cambridge, Mass., 1964.
7. D. L. MACADAM (Ed.), *Sources of Color Science*, M.I.T. Press, Cambridge, Mass., 1970.
8. C. S. BRINDLEY, *Physiology of the retina and visual pathway*, Monograph No. 6 of the Physiological Society, Edward Arnold Ltd., London, 1960.
9. A. C. HARDY (Ed.), *The Handbook of Colorimetry*, M.I.T. Press, Cambridge, Mass., 1936.
10. E. H. LAND, Experiments in Color Vision, *Scientific American*, May 1959.
11. J. Y. LETTVIN, The color of colored things, Quarterly Progress Report, 87, Research Laboratory for Electronics, M.I.T., Cambridge, Mass., 1967.
12. H. HELSON, Fundamental problems in color vision. I, *J. Exper. Psychol.* **23**, 1938.
13. H. HELSON, Fundamental problems in color vision. II, *J. Exper. Psychol.* **26**, 1940.
14. D. B. JUDD, Hue, saturation and lightness of surface colors with chromatic illumination, *J. Opt. Soc. Am.* **30**, 1940.
15. D. B. JUDD, *Color in Business, Science and Industry*, Wiley, New York, 1952.
16. W. RICHARDS, One-stage Model for Color Conversion, *J. Opt. Soc.* **62**, 1971.
17. E. H. LAND, The Retinex, *Am. Scientist*, **52**, 1964.
18. E. H. LAND AND J. J. MCCANN, Lightness Theory, *J. Opt. Soc.* **61**, 1971.
19. B. K. P. HORN, Shape from shading: A method for obtaining the shape of a smooth opaque object from one view, AI-TR-232, A.I. Laboratory, M.I.T., Cambridge, Mass., 1970.

20. R. D. RICHTMEYER AND K. W. MORTON, *Difference Methods for Initial Value Problems*, Wiley, New York, 1957.
21. D. R. GARABEDIAN, *Partial Differential Equations*, Wiley, New York, 1964.
22. B. K. P. HORN, The application of fourier transform methods to image processing, S. M. Thesis, E. E. Department, M.I.T., Cambridge, Mass., pp. 81–87 and 93–94, 1968.
23. T. CORNSWEET, *Visual Perception*, Academic Press, New York, 1970.
24. D. MARR, The computation of lightness by the primate retina, *Vision Research* 14, in press.